NASA Technical Memorandum 107375

# Sulfur Impurities and the Microstructure of Alumina Scales

James L. Smialek
*Lewis Research Center*
*Cleveland, Ohio*

Prepared for
Microscopy of Oxidation III
sponsored by the Institute of Metals
Cambridge, United Kingdom, September 16–18, 1996

Revised Copy

National Aeronautics and
Space Administration

# SULFUR IMPURITIES AND THE MICROSTRUCTURE OF ALUMINA SCALES

James L. Smialek
National Aeronautics and Space Administration
Lewis Research Center
Cleveland, Ohio 44135

## ABSTRACT

The relationship between the microstructure of alumina scales, adhesion, and sulfur content was examined through a series of nickel alloys oxidized in 1100 to 1200 °C cyclic or isothermal exposures in air. In cyclic tests of undoped NiCrAl, adhesion was produced when the sulfur content was reduced, without any change in scale microstructure. Although interfacial voids were not observed in cyclic tests of NiCrAl, they were promoted by long-term isothermal exposures, by sulfur doping, and in most exposures of NiAl. Two single crystal superalloys, PWA 1480 and Rene' N5, were also tested, either in the as-received condition or after the sulfur content had been reduced to <1 ppmw by hydrogen annealing. The unannealed alloys always exhibited spalling to bare metal, but interfacial voids were not observed consistently. Desulfurized PWA 1480 and Rene' N5 exhibited remarkable adhesion and no voidage for either isothermal or cyclic exposures. The most consistent microstructural feature was that, for the cases where voids did form, the scale undersides exhibited corresponding areas with ridged oxide grain boundaries. Voids were not required for spallation nor were other microstructural features essential for adhesion. These observations are consistent with the model whereby scale spallation is controlled primarily by interfacial sulfur segregation and the consequent degradation of oxide-metal bonding.

## INTRODUCTION

The adhesion of alumina scales on Ni(Co,Fe)CrAl alloys has been widely discussed in terms of micro–structural changes that occur concurrently with reactive element additions. Many of the proposed adhesion mechanisms were based on these microstructural features (ref. 1). However a decade ago the sulfur effect was introduced, according to which adhesion is related to interfacial segregation of sulfur, in contrast to the previous mechanisms all founded in microstructure: pegging, growth stress, vacancy sink, or scale plasticity (ref. 2). The critical role of the reactive elements is to getter sulfur impurities and prevent interfacial segregation. To test this mechanism, a number of studies attempted to produce some measure of adhesion, **without** reactive elements, by only reducing the sulfur content. If effective, this strategy would preclude other mechanisms based on the microstructural changes coincident with reactive element additions. Some early success was achieved for model NiCrAl alloys (refs. 3 and 4). Similar studies have shown the effectiveness of hydrogen annealing in reducing sulfur and producing adherent chromia scales on pure Cr (refs. 5 and 6).

Much subsequent low sulfur work concentrated on oxidation resistant single crystal superalloys. Here hydrogen annealing was used to remove sulfur to very low levels and produce excellent scale adhesion, to the point of being commercially significant (refs. 7 to 16). Generally these studies addressed the relationships between sulfur level, weight change, and segregation. Some microstructural features resulting from cyclic oxidation have been presented, but were generally too complex to allow direct comparisons between adherent and non-adherent $Al_2O_3$ scales (refs. 8 and 15). Accordingly, the purpose of the present review is to document whether obvious changes in $Al_2O_3$ microstructure necessarily accompany changes in $Al_2O_3$ adherence. In contrast to many previous studies relating microstructure to adhesion, here adherence was altered only by removing or adding sulfur, usually without any reactive elements present.

### Experimental Procedure

Model Ni-15Cr-24Al and Ni-50Al (at%) alloys were produced by arc melting buttons and subsequent drop casting into 1.2×l.2×5.0 cm ingots. Various levels of sulfur doping (10 to 1000 ppma) and zirconium doping (500 to 3000 ppma) were used for singly and co-doped compositions. Commercial superalloy stock was obtained for PWA 1480 and Rene'N5 (without Y). Oxidation coupons were approximately 0.l×l.2×l.2 cm. Sulfur reduction for NiCrAl (to 3 ppma) was achieved via repeated 1 hr oxidation at 1120 °C and light sanding with number 600 grit emery (ref. 3). Alternatively, sulfur removal to <1 ppma was achieved by hydrogen annealing in 100 percent $H_2$ or 5 percent $H_2$-Ar for 100 hr at 1200 °C. Previously published cyclic oxidation treatments of

these materials were at 1100 to 1150 ºC for times ranging from 200 to 1500 hr. The present study compares the microstructures obtained by a single 100 hr exposure in air at 1200 ºC for a number of the model alloys and the two superalloys.

## RESULTS

I. NiCrAl. The 1120ºC oxidation/polishing study of NiCrAl showed that about 10 cycles were required to produce an adherent scale and that 25 cycles achieved a sulfur reduction from the initial 15 ppma down to about 3 ppma. The scale structure and interfacial morphology were virtually unchanged from the first 1 hr cycle to the 25$^{th}$ 1-hr cycle, despite a global transformation from scales that spalled entirely to bare metal to scales that exhibited little, if any, spallation. Notable features were striations on the outermost (gas) surface, indicating some transient Ni,Cr-containing oxide, oxide grain imprints in the metal after spallation, and no apparent interfacial porosity (refs. 3 and 17). Continued cycling of the control sample, however, did eventually reduce the surface aluminum content sufficiently to allow colonies of coarse-grained Ni,Cr-rich spinels to form.

Sulfur reduction by hydrogen annealing improved the 1100 ºC cyclic oxidation behavior; the 200 hr weight loss was reduced from 24 mg/cm$^2$ to just 3 mg/cm$^2$. However, complete scale spallation was still observed after the 100 hr, 1200 ºC isothermal exposure. Hydrogen annealing was an effective desulfurization process (Table I), yet adhesion was not optimized for the cyclic test and not improved for the isothermal test.

Intentional sulfur doping increased the rate of weight loss in 1100 ºC cyclic tests. Spallation was even initiated by adding 100-1000 ppma S to the otherwise adherent NiCrAl+0.1 percent Zr system (ref. 18). Increased spallation resulted in complex, segmented scale structures, with aggregates of various Ni or Cr-rich oxides after 200 1 hr cycles. However, after only 10 cycles, the structures were sufficiently uncomplicated to distinguish bare metal, without voids, and intact alumina areas that resembled those on the NiCrAl+0.1 percent Zr base alloy. Thus interfacial voids were not a prevalent feature for frequently cycled NiCrAl oxidized at 1100 ºC.

However, a single long-time, higher temperature exposure did encourage interfacial voids. Figure 1 shows the microstructures of the exposed bare metal and the underside of the spalled scale for a NiCrAl+1000 S (ppma) sample oxidized at 1200 ºC for 100 hr. Oxide imprints are seen over much of the metal surface along with a high concentration of relatively smooth cavities. The corresponding oxide surface exhibits a dimpled grain structure over the area where voids exist in the metal. These areas were often associated with small Cr,S-rich particles, identified in the as-cast material as Cr(Ni)S by microprobe analyses. They were probably instrumental in the nucleation and growth of interfacial cavities (refs. 19 to 21). Higher magnification of the spalled scale underside (fig. 2) reveals very regular alumina grains (fig. 2(a)) that were in contact with the metal (imprints) and a grain boundary ridge morphology (dimples) grown over the void regions (fig. 2(b)), presumably by preferential inward oxygen grain boundary diffusion. The outer scale surface was a porous or dimpled structure and the cross-section was equiaxed.

II. NiAl. The microstructures formed by oxidation of β-NiAl are rich in variety and have been widely studied. Crystallographically faceted interfacial voids have been a predominant feature and dimpled or porous oxides exist over these cavities. These features were observed in most tests of undoped NiAl, whether cyclic or isothermal (ref. 22). Imprinted metal and ridged scale morphologies, similar to those for NiCrAl, were observed for isothermal 1200 ºC/100 hr exposure of undoped NiAl. Additionally, some of the grain imprints in the metal contained a central protrusion that appeared to correspond to frequent central cavities observed in those few oxide grains contacting the metal.

Doping with 100 ppma sulfur resulted in accelerated spallation in 1200 ºC cyclic tests, as might be expected. However, a loose and somewhat friable alumina scale remained on the sample in interrupted isothermal tests, exhibiting linear kinetics and a remarkably large weight gain of 50 mg/cm$^2$ after 500 hr. The scale was easily stripped, revealing extensive void areas, deep metal grain boundary cavities, and few isolated contact areas (oxide imprints), figure 3. The scale underside consisted almost entirely of the ridged grain boundary (dimpled) structure associated with noncontact regions. It was excessively convoluted with only the lowest points of the convolutions exhibiting a granular appearance (contact regions). The pores at the gas surface of the scale were coarser than those formed on undoped NiAl. However, the webbed ridge networks observed on the oxidized surface of Zr-doped NiCrAl, resulting from the θ-α transformation, are an order of magnitude coarser than the dimpled ridge structures formed on undoped or sulfur-doped NiAl.

Ill. PWA1480. Figure 4 shows the effect of sulfur content on the final weight change of PWA 1480 coupons after 500 hr of cyclic oxidation at 1100 ºC. The sulfur content was adjusted by hydrogen annealing over a test matrix of various times, temperature, and sample thicknesses. The as-received samples, having an initial sulfur level of about 6 ppmw (10 ppma), all showed a considerable degree of distress (20 to 70 mg/cm$^2$

weight loss). As the sulfur level was reduced to below 1 ppmw, spalling was markedly reduced. At about 0.3 ppmw or below, spalling was essentially eliminated, with nearly all of these samples maintaining positive weight changes out to 1000 hr.

The scale phases were primarily $Al_2O_3$, $NiCr_2O_4$, and $CrTaO_4$. The more adherent scales contained primarily the Al-rich phases, whereas the less adherent scales exhibited a predominance of the Ni,Cr-rich phases. This transition to Ni,Cr-rich oxides occurred after repeated cycles of alumina spallation, re-growth, and aluminum depletion. The unannealed sample revealed a complex mosaic of Ni, Cr, or Ta-rich oxide nodules after 500 cycles, impinging or overgrowing the remnants of an alumina base scale. The areas of spalling to bare metal were well dispersed, but limited in width to only about 50 micrometers. These areas were totally depleted of aluminum (EDS), contained distinct imprints of the oxide grains, but exhibited no voids. In contrast the adherent scale on hydrogen annealed PWA 1480 (1200 $^{o}$C for 100 hr) exhibited a very uniform, fine grain, Al-rich surface, only rare patches of spalling to bare metal, and again no voids (oxidized at 1100 $^{o}$C for 1000 cycles).

A more discriminating comparison was evident after the single 1200 $^{o}$C, 100 hr exposure. Here both as-received and hydrogen annealed specimens grew primarily alumina scales. Both surfaces exhibited similar fine grained nodules (fig. 5). However, on cooling, the scale spalled off essentially the entire as-received speci–men, while the scale on the hydrogen annealed sample (less a few local areas) remained quite intact (fig. 6). The bare metal regions of both samples exhibited identical oxide grain imprint structures (grain sizes). However only the as-received sample exhibited an appreciable amount of large, smooth, interface voids - again associated with dimpled convoluted regions of the oxide underside.

The contrast between cyclic and isothermal exposures suggests that repeated spallation and regrowth of alumina was responsible for aluminum depletion and the transition to more Ni, Cr, or Ta-rich phases for the unannealed sample. Void formation was not observed and was not necessary for spallation in the cyclic test, but occurred quite noticeably in the isothermal test. Hydrogen annealing produced adherent scales in both cyclic and isothermal tests, while curtailing void formation in the isothermal test.

IV. Rene' N5. Cyclic oxidation of Rene' N5 (without Y) at 1150 $^{o}$C resulted in performance and micro-structural effects similar to those of PWA 1480. The unannealed sample lost 24 mg/cm$^2$ after 500 hr and produced a complex multiphase scale (figure 7). In contrast, a sample that was hydrogen annealed (1280 $^{o}$C for 100 hr) gained only 1 mg/cm$^2$ after 1000 hr cyclic oxidation at 1150 $^{o}$C and produced a uniform scale with no spalling to bare metal. SEM/EDS and XRD analyses produced results similar to that of PWA 1480, except that the evidence for the $NiTa_2O_4$ phase was stronger than that for the $CrTaO_4$ phase having a similar rutile structure.

The isothermal exposure again allowed more direct comparisons. The scale surfaces both consisted of fine granular nodules. Bare metal regions exhibited oxide grain imprints exclusively (no voids) in all the areas examined of both samples. For the as-received coupon, a number of 20 micrometer pits were observed. But these pits also contained imprints or remnants of Al-rich oxide protrusions. The only indication that void formation may have occurred was the observation of a localized array of open cavities with free standing alumina crystals in the underside of one spall fragment (fig. 8(a)). The cross section of another spall fragment revealed primarily a columnar growth structure (fig. 8(b)), which has often been associated with adherent scales.

Where spalling did occur on the flat surface of the hydrogen annealed Rene'N5 sample, the extent was never to bare metal. The only region exhibiting oxide imprints and bare metal spalling was the edge of the hanger hole where the thermal expansion mismatch stresses would be the highest. No voids were observed in this spalled region.

## DISCUSSION

A rich diversity of scale structures was shown to form on a number of different alloys having sulfur levels characterized as either nominal (as-received at 5 to 15 ppm), high (intentionally doped to 100 to 1000 ppm), or low (desulfurized to <1 ppm). The results of the single (long term) isothermal exposure are summarized in Table I for ease of comparison. The general behavior is outlined below.

The short time adherent scales formed on purged NiCrAl were indistinguishable from those on the con–ventionally cycled sample that exhibited spalling. Intentional sulfur doping did increase cavity formation on NiCrAl for the higher temperature isothermal test. Porous or dimpled surface scales were common for undoped and sulfur doped NiAl and NiCrAl. Interfacial voids in the metal were prevalent for the undoped and sulfur-doped NiAl cases, but were non-existent for undoped NiCrAl in cyclic tests. These cavity areas were typically associated with grain boundary ridged structures in the corresponding underside of spalled scales.

Furthermore, removing sulfur from the single crystal superalloys caused a remarkable increase in scale adhesion in cyclic tests without an apparent change in the scale morphology. While adhesion is produced by reducing the sulfur content below 1 ppm, the alumina scale morphology is not changed for these desulfurized samples. It is therefore difficult to support adhesion mechanisms rooted primarily in scale morphology pheno–mena. The controlling mechanism is therefore now believed to be related to interfacial chemistry and not to scale morphology, as had previously been the case for many reactive element mechanisms. Sulfur segregation at free surfaces and the alumina-metal interface has been widely observed (refs. 2, 10, 15, 19, 20, and 23 to 33).

One of the goals of the present program is to define a critical sulfur content, below which no additional adhesion benefit is obtained. A criterion was proposed to define this level, based on the number of monolayers of sulfur that could possibly segregate, given the impurity level and the dimensions of the sample (refs. 12, 16, and 17). Generally, the cyclic oxidation performance reaches its ultimate at about 0.3 ppmw sulfur (refs. 16 and 17).

A summary of the performance of bulk sulfur single crystal superalloys, given on the so-called adhesion map of figure 9, indicates that excellent performance is obtained if the total equivalent sulfur content is equal to or less than about one monolayer. There are three related reasons why this may be so:

1. A low bulk sulfur content limits the total segregation possible.

2. The reduced amount lowers the diffusional supply in a cyclic test, where a continuous supply of sulfur might be required to cause repeated spallation.

3. The low bulk amounts also reduce the segregation level in equilibrium with the bulk sulfur activity (refs. 7, 12, and 23).

The criticality of monolayer levels of bulk sulfur is related to the fact that nickel alloy surfaces are saturated at only 0.3-0.5 monolayers of sulfur (refs. 23 to 25). Therefore a bulk sulfur content equivalent to a few saturated interfaces is believed to be sufficient to cause repeated spallation, aluminum depletion, and to trigger further degradation through non-protective scale formation.

## CONCLUDING REMARKS

This study has provided a cursory look at a potpourri of scale structures grown on alumina-forming alloys. Intentional sulfur **doping** and long term, higher temperature isothermal exposures did encourage more scale detachment, deformation, interfacial cavities and related features, such as grain boundary ridges on the scale underside. However, sulfur **removal** did not consistently alter microstructure while imparting adhesion in either cyclic or isothermal tests. While morphological changes may accompany changes in scale adhesion for some cases, they are not a necessary prerequisite for adhesion in general. The overall perspective gained from this study leads toward increased emphasis on interfacial segregation of sulfur as the primary factor causing spallation, with scale morphology and associated mechanisms as secondary components.

## REFERENCES


1. D.P. Whittle and J. Stringer: ‘Improvements in Properties:Additives in Oxidation Resistance’, *Phil. Trans. Royal Soc. A*, **295**, 309-329, 1980.
2. J.G. Smeggil, A.W. Funkenbusch, and N.S. Bornstein: ‘A Relationship between Indigeneous Impurity Elements and Protective Oxide Scale Adherence Characteristics’, *Metall. Trans*., Vol **17A**, 923-932, 1986.
3. J.L. Smialek: ‘Adherent $Al_2O_3$ Scales Produced on Undoped NiCrAl Alloys’, *Metall. Trans.*, 18A, 164-167, 1987; also in *Oxidation of Metals and Associated Mass Transfer*, M.A. Dayanada, S.J. Rothman, and W.E. King, eds., *TMS-AIME*, Warrendale, PA, 297-313, 1987.
4. J.G. Smeggil: ‘Some Comments on the Role of Y in Protective Oxide Scale Adherence’, *Mater. Sci. and Engineer*., **87**, 261-265, 1987.
5. D.G. Lees: ‘On the Reasons for the Effects of Dispersions of Stable Oxides and Additions of Reactive Elements on the Adhesion and Growth Mechanisms of Chromia and Alumina Scales - the Sulfur Effect’, *Oxidation of Metals*, **27**, 75-81, 1987.

6. I. Melas and D.G. Lees: 'Factors affecting adhesion of chromia scales on chromium', *Mat. Sci. and Techn.*, 455-456, 1988.
7. J.L. Smialek: 'The effect of sulfur content on $Al_2O_3$ scale adhesion', in *Microscopy of Oxidation 1*, M.J. Bennett and J. Lorimer, eds., Institute of Metals, London, 258-270, 1990.
8. B.K. Tubbs and J.L. Smialek: 'Effect of Sulfur Removal on Scale Adhesion to PWA 1480', in *Corrosion and Particle Erosion at High Temperatures*, V. Srinivasan and K. Vedula, eds., TMS-AIME, Warrendale, PA, 459-487, 1989; also J.L. Smialek and B.K. Tubbs, *Metall. and Mat. Trans.*, **26A**, 427-435, 1995.
9. R.V. McVay, P. Williams, G.H. Meier, F.S. Pettit, and J.L. Smialek: 'Oxidation of Low Sulfur Single Crystal Nickel-Base Superalloys', in *Superalloys 1992*, S.D. Antolovich et al., eds., TMS-AIME, Warrendale, PA, 807-816, 1992.
10. D.T. Jayne and J.L. Smialek: 'A Sulfur Segregation Study of PWA 1480, NiCrAl, and NiAl Using X-ray Photoelectron Spectroscopy with in-situ Sample Heating', in *Microscopy of Oxidation 2*, S.B. Newcomb and M.J. Bennett, eds., Institute of Materials, London, 183-196, 1993.
11. W.P Allen, N.S. Bornstein, S. Chin, M. DeCrescente, D.N. Duhl, R.A. Pike, and J.G. Smeggil, 'Method for Removing Sulfur from Superalloy Articles to Improve Their Oxidation Resistance'; U.S. Patent 5,346,563, Sept. 13, 1994.
12. J.L. Smialek, D.T. Jayne, J.C. Schaeffer, and W.C. Murphy: 'Effect of hydrogen annealing, sulfur segregation and diffusion on the cyclic oxidation resistance of superalloys: a review', *Thin Solid Films*, **253**, 285-292, 1994.
13. G.H. Meier, F.S. Pettit, and J.L. Smialek: 'The Effects of Reactive Element Additions and Sulfur Removal on the Adherence of Alumina to Ni- and Fe-Base Alloys', *Werkstoffe und Korrosion*, **46**, 232-240, 1995.
14. J.C. Schaeffer, W.C. Murphy, and J.L. Smialek, 'The Effect of Surface Condition and Sulfur on the Environmental Resistance of Airfoils', *Oxid. Met.*, **43**, 1995.
15. M. A. Smith, W.E. Frazier, and B.A. Pregger: 'Effect of Sulfur on the Cyclic Oxidation Behavior of a Single Crystalline Nickel-Based Superalloy', *Mat. Sci. and Engineer*., **203**, 388-398, 1995.
16. J.L. Smialek: 'Oxidation Resistance and Critical Sulfur Content of Single Crystal Superalloys', ASME paper 96-GT-519, 1-7, 1996; (presented at the IGTI TurboExpo '96, Birmingham, U.K. , June 10-13, 1996).
17. J. L. Smialek: 'Effect of Sulfur Removal on $Al_2O_3$ Scale Adhesion', in *Corrosion and Particle Erosion at High Temperatures*, V. Srinivasan and K. Vedula, eds., TMS-AIME, Warrendale, PA, 425-458, 1989, also J.L. Smialek, *Metall. Trans*., 22A, 739-752., 1991.
18. J.L. Smialek: 'Effect of Sulfur and Zirconium Co-doping on the Oxidation of NiCrAl', *High Temp. Mat. Chem. IV*, Z.A. Munir, D. Cubicciotti, and H. Tagawa, eds., The Electrochem. Soc., Pennington, NJ, 241-253, 1988.
19. H.J. Grabke, D. Wiemer, and H. Viefhaus: 'Segregation of sulfur during growth of oxide scales', *Appl. Surf. Sci.*, **47**, 243-250, 1991.
20. H.J. Grabke, G. Kurbatov, and H.J. Schmutzler: 'Segregation beneath Oxide Scales', *Oxid. Met.*, **43**, 97-115, 1995.
21. B. Pint, 'On the Formation of Interfacial and Internal Voids in $\alpha$-$Al_2O_3$ Scales', submitted to *Oxid. Met., 1996.*
22. J.L. Smialek: 'Oxide Morphology and Spalling Model for NiAl', *Metall. Trans.*, **9A**, 309-320, 1978.
23. Miyahara, K. Stolt, D.A. Reed, and H.K. Birnbaum: 'Sulfur Segregation on Nickel', *Scripta Met*., **19**, 117-121,1985.
24. J.L. Smialek and R. Browning: 'Current Viewpoints on Oxide Adherence Mechanisms', in *High Temperature Materials Chemistry III*, R. Rapp, ed., The Electrochemical Society, Pennington, NJ, pp. 259-271, 1986; also NASA TM 87168, 1985.
25. Walker and M.M. El Gomati: 'On the Role of Zirconium and Sulfur in the Oxidation of a Doped Superalloy', *Appl. Surf. Sci*., **35**, 164, 1988-89.
26. P.Y. Hou and J.Stringer: 'Observation of oxide/metal interface using scanning Auger microscopy with an in-situ scratch technique', in *Microscopy of Oxidation 1*, M.J. Bennett and J. Lorimer, eds., Intistitute of Metals, London, 362-368, 1990.
27. P.Y. Hou and J. Stringer: 'Oxide Scale Adhesion and Impurity Segregation at the Scale Metal Interface', *Oxid. Met*, **83**, 323-345, 1992.
28. P.Y. Hou, K.B. Alexander, K. Prussner, and Z. Wang: 'Sulfur Segregation to Oxide/Metal Interfaces: a Comparison of Thermally Grown and Plasma Deposited $Al_2O_3$', *Microscopy of Oxidation 3*, S.B. Newcomb and J.A. Little, eds., Institute of Materials, London, 1996.

29. H. Grabke and H. Viefhaus, ‘Application of LEED and auger electron spectroscopy in the study of high temperature corrosion mechanisms’, in *Microscopy of Oxidation 1*, M.J. Bennett and J. Lorimer, eds., Institute of Metals, London, 19-33, 1990.
30. G. Tatlock, P.G. Beahan, J. Ritherdon, and A. Partridge: ‘The Oxidation of Nickel-based Alloys Containing Sulfur’, in *Microscopy of Oxidation 2*, S.B. Newcomb and M.J. Bennett, eds., Institute of Materials, London, 172-182, 1993.
31. R. Dennert, H.J. Grabke, and H. Viefhaus: ‘Effect of Sulfur in the Initial Stage of Oxidation of Ni-20Cr Single Crystals’, in *Microscopy of Oxidation 2*, S.B. Newcomb and M.J. Bennett, eds., Institute of Materials, London, 197-204, 1993.
32. C.L. Briant, W.H. Murphy, and J.C. Schaeffer: ‘The Effect of Annealing and Desulfurization on Oxide Spallation of Turbine Airfoil Material’, *Scripta Met. et Mat.*, **32**, 1447-1451, 1995.
33. A. Glaskov, M. Gobel, G. Borchardt, H. Al-Badairy, J. Ritherdon, G.J. Tatlock, and J. LeCoze: ‘An Auger Study of the Composition of the Metal-Oxide Interface in Fe-20Cr-5Al Based Alloys Revealed by Bending Experiments under UHV Conditions’, in *Microscopy of Oxidation 3*, S.B. Newcomb and J.A. Little, eds., Institute of Materials, London,1996.

TABLE I.—SUMMARY OF MORPHOLOGICAL FEATURES FOR ALUMINA SCALES FORMED ON VARIOUS ALLOYS BY A SINGLE OXIDATION EXPOSURE AT 1200 $^{O}$C FOR 100 hr

| Alloy | Condition | S, ppma | mg/cm$^2$ | Overall | Detailed structure |
|---|---|---|---|---|---|
| NiCrAl | as-received | 40 | -1.60 | spalled | convoluted, no voids |
| | $H_2$-annealed | 0.03 | -1.02 | spalled | convoluted, no voids |
| | S-doped | 1000 | -2.47 | spalled | convoluted, 20% voids + g.b ridges, equiaxed, |
| | Zr-doped | 40 | +1.11 | adherent | |
| NiAl | as-received | 1.7 | +0.26 | spalled | convoluted, 50% voids + g.b. ridges, equiaxed |
| | S-doped | 140 | +2.70 | loose | wrinkled, 100% voids + g.b. ridges |
| | Zr-doped | 1.7 | +1.83 | adherent | |
| 1480 | as-received | 10 | -1.35 | spalled | local wrinkles, g.b. ridges and 40 percent voids (rest void-free), columnar |
| | $H_2$-annealed | 0.1 | +2.66 | adherent | no voids |
| N5 | as-received | 5.1 | -1.14 | spalled | local convolutions, no voids |
| | $H_2$-annealed | 0.5 | +0.82 | adherent | no voids |
| | Y-doped | 5.1 | +0.91 | adherent | |

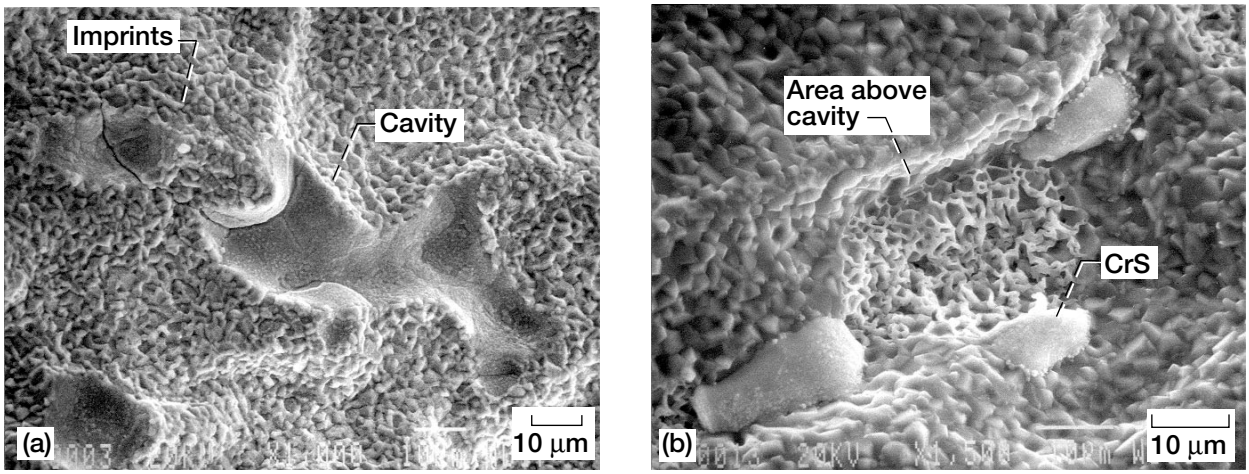


Figure 1.—Microstructure of NiCrAl+1000 ppma S after 100 hr isothermal oxidation at 1200 °C. (a) Metal exposed by spalling, showing smooth cavities and textured imprints of oxide grains. (b) Underside of spalled oxide showing granular structure, dimpled grains, and associated sulfide particles.

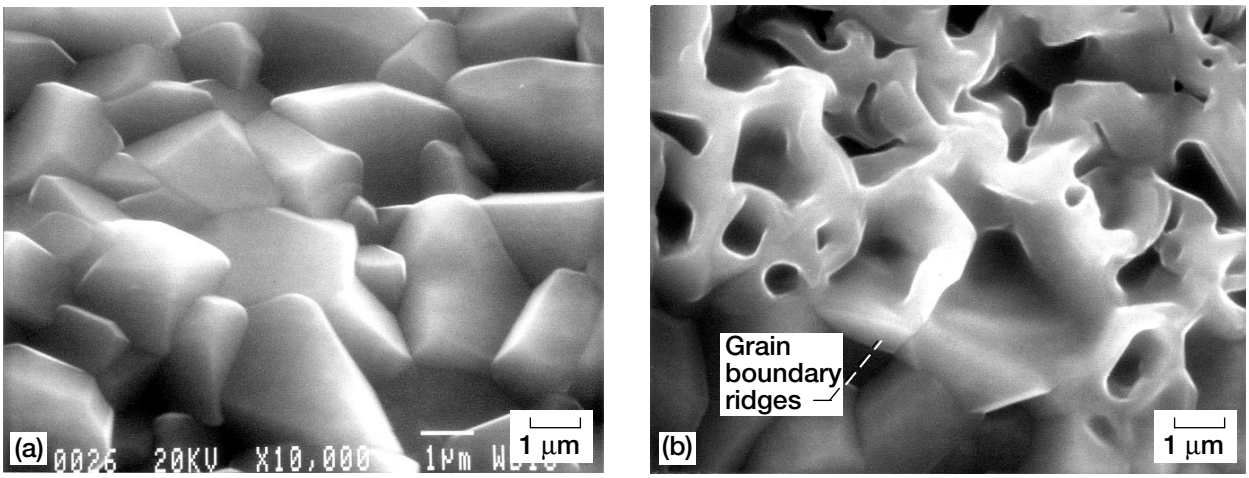


Figure 2.—Details of figure 1(b) showing (a) regular alumina grains (metal contact area), and (b) grain boundary ridges in dimpled oxide grown over interfacial cavities.

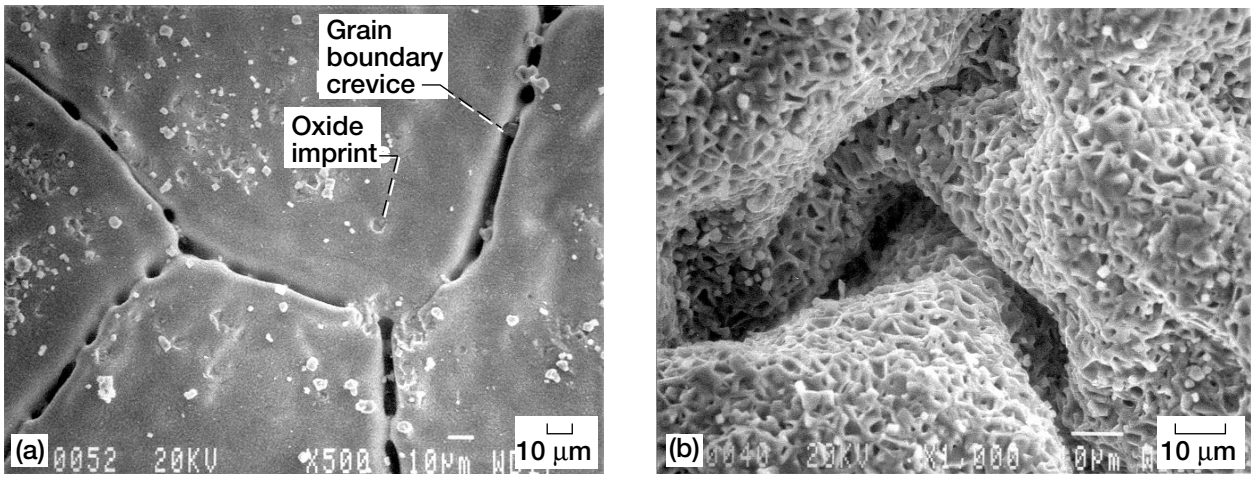


Figure 3.—Microstructure of NiAl + 100 ppma S after 100 hr isothermal oxidation at 1200 °C. (a) Exposed metal showing extensive smooth (voided) regions, preferential metal grain boundary cavities, and sparse imprints or oxide grains; (b) excessive deformation and dimpled structure of spalled oxide underside.

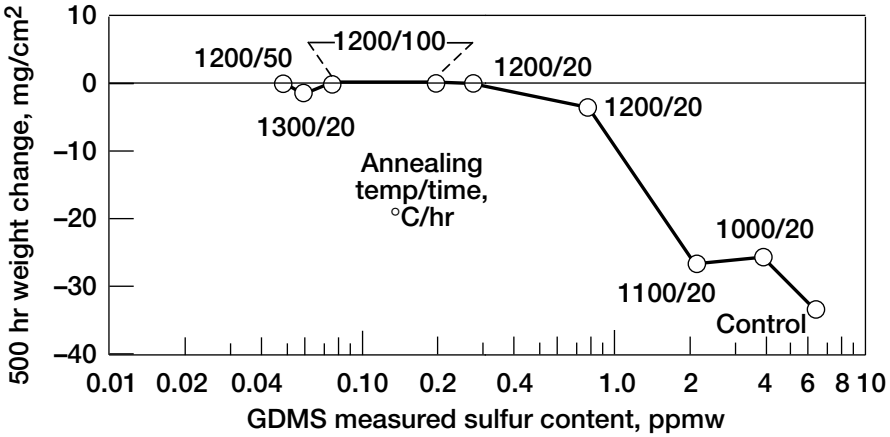


Figure 4.—The effect of alloy sulfur content on the 500 hr final weight change for PWA 1480, hydrogen annealed to various sulfur levels and oxidized at 1100 °C using 1-hr cycles.

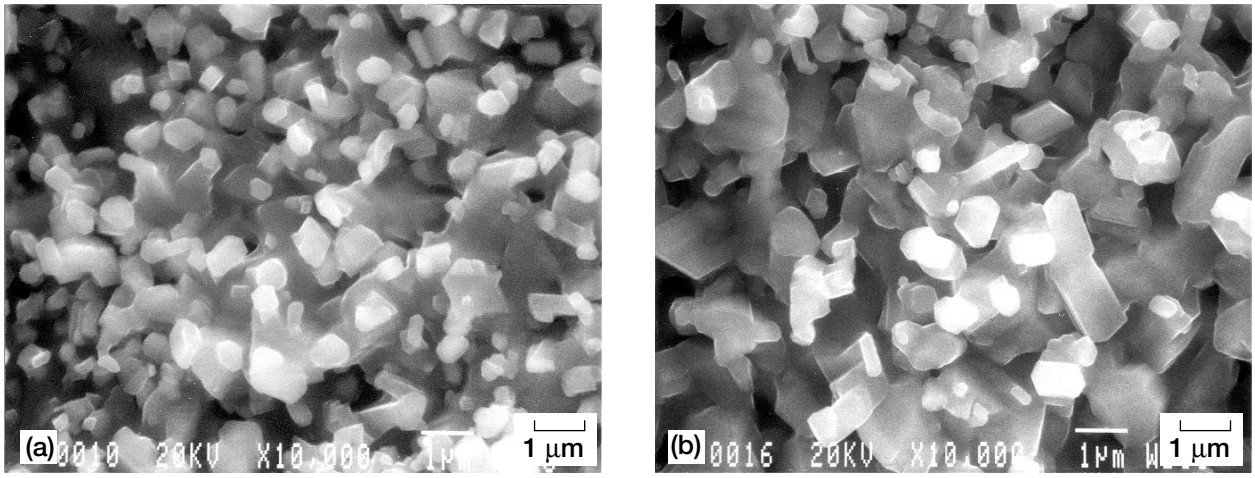


Figure 5.—Similar surface scale morphology for PWA 1480 after 100 hr isothermal oxidation at 1200 °C. (a) Tested as-received, sulfur content (6 ppmw); (b) tested after hydrogen annealing for 100 hr at 1200 °C, desulfurized to 0.1 ppmw.

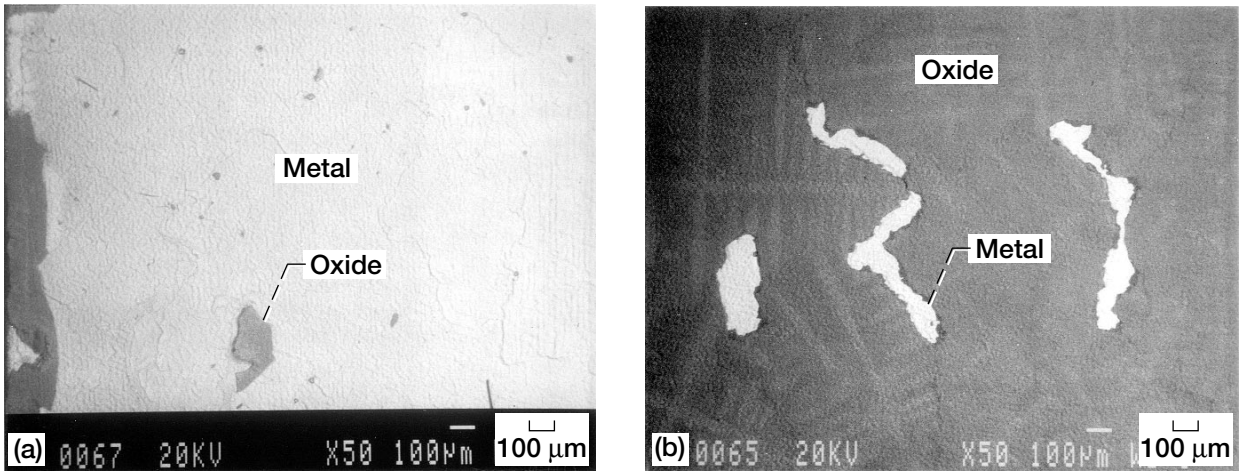


Figure 6.—Backscatter SEM images showing (a) extensive and (b) minimal loss of scale for the as-received and hydrogen annealed samples of figure 5.

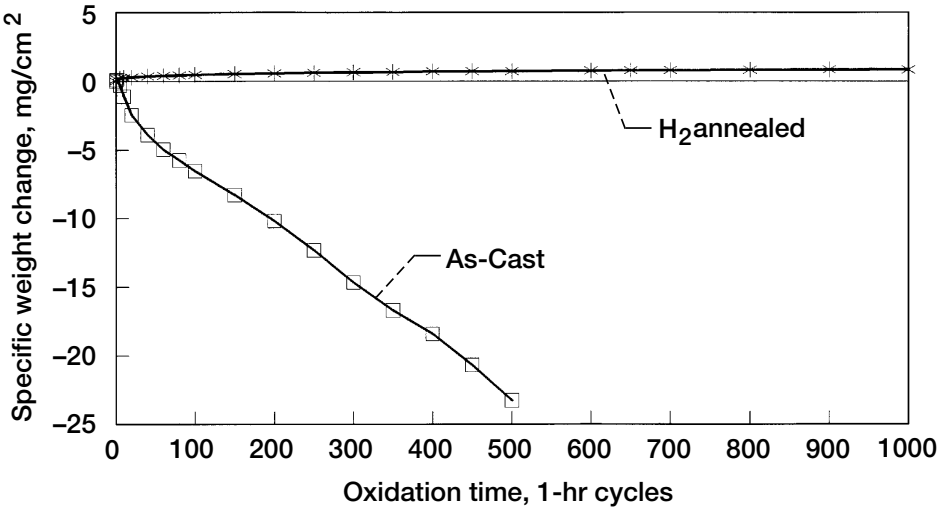


Figure 7.—1150 °C cyclic oxidation behavior of Rene'N5 superalloy (without Y), as-received and hydrogen annealed (1280 °C for 100 hr); [from ref. 12].

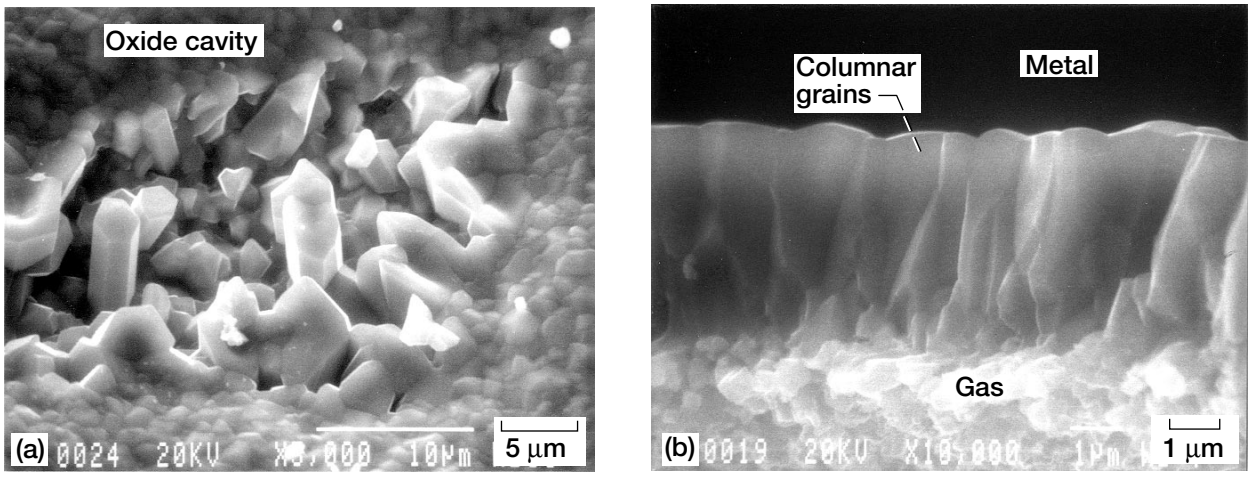


Figure 8.—Spalled scale microstructure of Rene'N5 after 100 hr isothermal oxidation at 1200 °C; (a) faceted alumina crystal growth in underside cavity; (b) cross-section showing columnar growth beneath a small equiaxed layer.

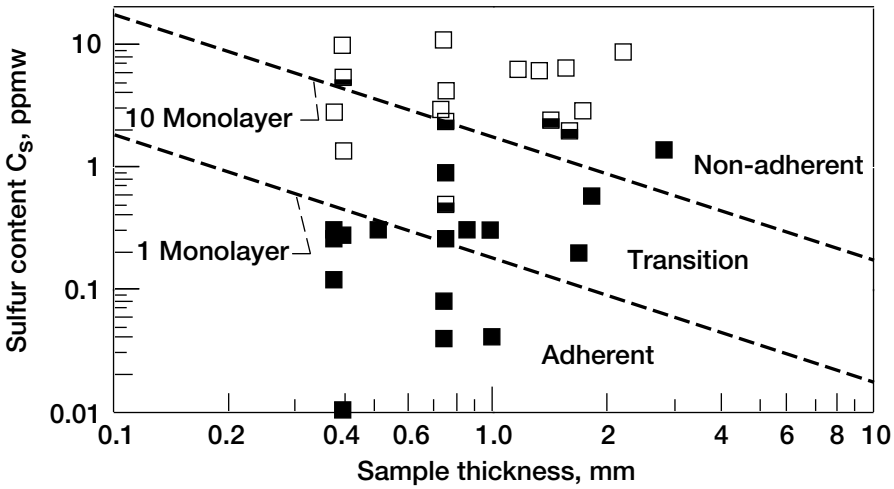


Figure 9.—Proposed adhesion map relating the adherent behavior (filled symbols) of desulfurized superalloys and the non-adherent behavior of as-received superalloys (open symbols) to the total number of segregated sulfur monolayers possible. The major transitions occur in the regime of a few monolayers and suggest critical sulfur contents <1 ppmw for typical airfoil thicknesses [from ref. 16].

# REPORT DOCUMENTATION PAGE

*Form Approved*
*OMB No. 0704-0188*



**1. AGENCY USE ONLY** (*Leave blank*)

**2. REPORT DATE**
April 1997

**3. REPORT TYPE AND DATES COVERED**
Technical Memorandum

**4. TITLE AND SUBTITLE**
Sulfur Impurities and the Microstructure of Alumina Scales

**5. FUNDING NUMBERS**
WU–523–21–13

**6. AUTHOR(S)**
James L. Smialek

**7. PERFORMING ORGANIZATION NAME(S) AND ADDRESS(ES)**
National Aeronautics and Space Administration
Lewis Research Center
Cleveland, Ohio 44135–3191

**8. PERFORMING ORGANIZATION REPORT NUMBER**
E–10544

**9. SPONSORING/MONITORING AGENCY NAME(S) AND ADDRESS(ES)**
National Aeronautics and Space Administration
Washington, DC 20546–0001

**10. SPONSORING/MONITORING AGENCY REPORT NUMBER**
NASA TM–107375
*Revised Copy*

**11. SUPPLEMENTARY NOTES**
Prepared for Microscopy of Oxidation III sponsored by the Institute of Metals, Cambridge, United Kingdom, September 16–18, 1996. Responsible person, James L. Smialek, organization code 5160, (216) 433–5500.

**12a. DISTRIBUTION/AVAILABILITY STATEMENT**
Unclassified - Unlimited
Subject Category 26

This publication is available from the NASA Center for AeroSpace Information, (301) 621–0390.

**12b. DISTRIBUTION CODE**

**13. ABSTRACT** ***(Maximum 200 words)***

The relationship between the microstructure of alumina scales, adhesion, and sulfur content was examined through a series of nickel alloys oxidized in 1100 to 1200 °C cyclic or isothermal exposures in air. In cyclic tests of undoped NiCrAl, adhesion was produced when the sulfur content was reduced, without any change in scale microstructure. Although interfacial voids were not observed in cyclic tests of NiCrAl, they were promoted by long-term isothermal exposures, by sulfur doping, and in most exposures of NiAl. Two single crystal superalloys, PWA 1480 and Rene' N5, were also tested, either in the as-received condition or after the sulfur content had been reduced to <1 ppmw by hydrogen annealing. The unannealed alloys always exhibited spalling to bare metal, but interfacial voids were not observed consistently. Desulfurized PWA 1480 and Rene' N5 exhibited remarkable adhesion and no voidage for either isothermal or cyclic exposures. The most consistent microstructural feature was that, for the cases where voids did form, the scale undersides exhibited corresponding areas with ridged oxide grain boundaries. Voids were not required for spallation nor were other microstructural features essential for adhesion. These observations are consistent with the model whereby scale spallation is controlled primarily by interfacial sulfur segregation and the consequent degradation of oxide-metal bonding.

**14. SUBJECT TERMS**
Oxidation; Sulfur; Alumina; Adhesion

**15. NUMBER OF PAGES**
14

**16. PRICE CODE**
A03

**17. SECURITY CLASSIFICATION OF REPORT**
Unclassified

**18. SECURITY CLASSIFICATION OF THIS PAGE**
Unclassified

**19. SECURITY CLASSIFICATION OF ABSTRACT**
Unclassified

**20. LIMITATION OF ABSTRACT**